Journal of Applied Electrochemistry **31**: 1273–1279, 2001.

Anodic oxidation behaviour of Al–Ti alloys in acidic media

Y. SONG, X. ZHU, X. WANG, J. CHE and Y. DU
Chemical Engineering Institute, Nanjing University of Science & Technology, Nanjing 210014, P.R. China
*(*author for correspondence, e-mail: soong_ye@sohu.com)*

Received 25 January 2001; accepted in revised form 25 July 2001

Key words: Al–Ti alloy, anodic oxidation, dielectric film, solid capacitor, surface analysis

Abstract

The anodic oxidation behaviour of Al–Ti alloys in several acidic solutions was investigated. The influence of conditions such as alloy composition, electrolytic solution, electrolyte temperature and formation current density on the formation rate of oxides on Al–Ti alloys and the dielectric properties of the anodic films were analysed. It was shown that the oxide formation rate for the Al–Ti alloy containing 54 at % aluminium was the highest and the dielectric property of its anodic oxide was also the best. In addition, by means of several surface analytical techniques, the chemical composition of the films were determined as $(TiO_2)_n(Al_2O_3)_m$. AES (Auger electron spectroscopy) profiling analysis data showed that Al–Ti alloys had preferential oxidation behaviour, that is, the aluminium was oxidized preferentially.

1. Introduction

It is well known that solid tantalum electrolytic capacitors occupy an important position in circuit applications due to their unsurpassed volumetric efficiency of capacitance and long life. These capacitors, however, have high cost per unit of capacitance because of their use of noble metal materials. In 1983, the NEC Corporation reported that an Al–Ti alloy solid electrolytic capacitor had been developed successfully [1]. It was claimed that this type of capacitor had comparable properties with tantalum electrolytic capacitors but that its cost was similar to that of aluminium capacitors. Anodic oxide films on a porous Al–Ti alloy body were used as a dielectric in this type of capacitor with large capacitance being provided due to extremely thin oxide layers and the high surface areas of porous Al–Ti alloys. Al–Ti alloy electrolytic capacitors have attracted considerable attention as a new type of solid capacitor. Although considerable effort has focused on fabricating methods of the capacitors [2, 3], there have been almost no reports of fundamental investigations of Al–Ti alloys employed as capacitor materials [4], though papers on anodic oxidation of pure valve metals such as aluminium abound [5–7]. To improve the properties of Al–Ti alloy capacitors, it is essential to obtain a clear understanding of the nature of anodic oxide films. In this paper we report the anodic oxidation behaviour of Al–Ti alloys in some acidic solutions.

2. Experimental details

Titanium samples were 99.992% purity foils, about 60 μm thick. The samples were cleaned in NaOH solutions, followed by an ultrasonic cleaning for about 10 min with acetone and ethanol respectively. Chemical polishing for about 5–8 s in solutions composed of HNO_3 (70%), H_2SO_4 (97%), HF (48%) and H_2O in a volume ratio of 2:1:1:1 was then carried out followed by a thorough rinse in deionized water.

Aluminium foils used were also 99.992% purity and about 100 μm thick. The processing of aluminium samples was the same as that of titanium but with a shorter time of chemical polishing (~3–4 s).

Al–Ti alloys used were made by smelting high purity aluminium powder (99.992%) and titanium powder (99.994%) at high temperature under vacuum environment. The alloys were provided in rod form with three compositions containing 36, 54 and 68 at % of aluminium (marked A, B and C, respectively). These rods were abraded with suspensions of diamond paste to a mirror finish. Prior to experiment, the polished samples were immersed in NaOH solutions (10 wt %) for about 2 min to remove natural surface oxide films, followed by ultrasonic cleaning for about 10 min with acetone and ethanol, respectively, and then a thorough rinse in deionized water. The samples were then mounted in resin to expose a square face, 1 cm × 1 cm in area, to the electrolytic solutions.

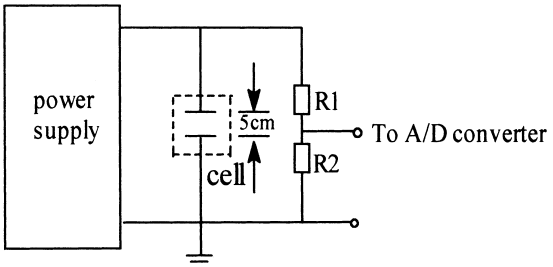

Fig. 1. Schematic representation of the measurement system for anodic oxidation.

The formation curves were recorded by obtaining the dependence of cell voltage, between anode and cathode, on time under galvanostatic anodizing conditions. Anodic oxidations of all samples were carried out at a constant applied current density of 1.5 mA cm^{-2}, except when otherwise stated. The forming electrolytes were mainly acidic solutions including phosphoric acid, boric acid, citric acid and sulfuric acid. To obtain automatic measurement of the formation curves, a system was established as shown in Figure 1. The space between the two electrodes was 5 cm. A power supply was used to provide a constant current. R_1 and R_2 are two resistors to sample cell voltage. An IBM PC computer with a PC-1216C A/D board was used to record the voltage while anodizing. The A/D converter board was 12 bit and had 16 channels, the sampling time was 100 μs. The measurement system recorded the voltage at a rate of one point per second.

The AES profiling analyses of the anodic oxide films were performed with a PHI600 Auger electron spectroscopy (AES) combined with a sample sectioning technique of 3 keV Ar^+ ion sputter. The chemical compositions of the anodic oxide were determined by X-ray photoelectron spectroscopy (XPS) using a PHI5400 spectrograph. The intermetallic phases of the alloys were investigated by X-ray diffraction (XRD) using a D/Max-IIIA automatic diffractometer with CuK_α radiation.

3. Results and discussion

3.1. *Alloy composition*

It is well known that the formation voltage of valve metals rises approximately linearly with time from the commencement of anodizing until dielectric breakdown under galvanostatic anodizing conditions [8]. Figure 2 shows formation curves for three alloy compositions (sample A, B, C) and pure titanium as well as pure aluminium in 0.01 vol % phosphoric acid at 298 K. The oxide formation property of pure titanium is very poor. During anodizing, its cell voltage maintained a rather low constant value or increased slowly with time accompanied by copious gas evolution. In the case of pure aluminium and Al–Ti alloy samples A, B, C, their formation voltages increased almost proportionally with

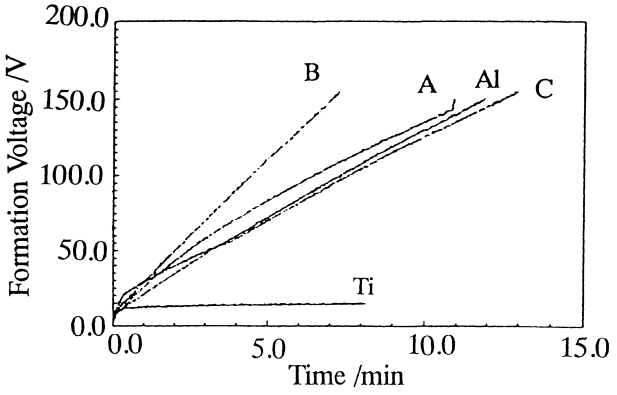

Fig. 2. The formation curves of Al–Ti alloy (sample A, B and C), pure aluminium and pure titanium in phosphoric solutions.

time up to about 150 V, while gas evolution on the anode samples was very slight. As shown in Figure 2, the slope, dV/dt, of the V/t curves is the greatest for alloy B, which indicates that the oxide formation rate on alloy B in phosphoric solutions is the fastest. In fact, the oxide formation rate is close related to alloy composition. Generally, the oxide formation rate of pure titanium is very low. For Al–Ti alloys, the rate increases initially with increasing aluminium content, and then reaches a maximum value with aluminium contents of about 54 at %, followed by a drop in rate with further increase in aluminium content. Anodizing parameters and the dielectric properties of the oxide films in phosphoric solutions are shown in Table 1. The final leakage current in Table 1 refers to the residual current through the cell after the samples had been anodised galvanostatically to 150 V and then kept at this voltage for 2 h.

Table 1 indicates that the formation behaviour changes with alloy composition and that sample B has the highest formation rate and the best insulating properties for its oxide films. Similar trends were observed in other acid-containing solutions as shown by the data presented in Figure 3.

In reality, the dependence of the oxide formation rate on alloy composition is directly related to various component phases. XRD results of samples A, B and C implied that the main component phases of the three alloys were different, namely, Ti_2Al, TiAl, $TiAl_3$ phase for samples A, B and C, respectively (Table 2). It is understood that these different intermetallic compounds should have different oxide formation rates during galvanostatic anodization. Generally, the anodic oxide

Table 1. Anodizing parameters for different alloy compositions and insulating properties of the resulting oxide films

Samples	Average formation rate/V min^{-1}	Final leakage current/μA (150 V for 2 h potentiostatic)
A(36 at % Al)	12.2	320
B(54 at % Al)	20.2	25
C(68 at % Al)	10.8	390

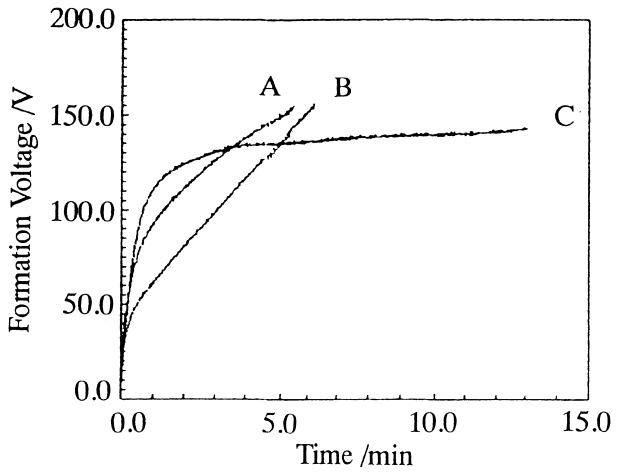

Fig. 3. Formation curves of Al–Ti alloy (sample A, B and C) in 0.2 M boric acid solutions at 298 K.

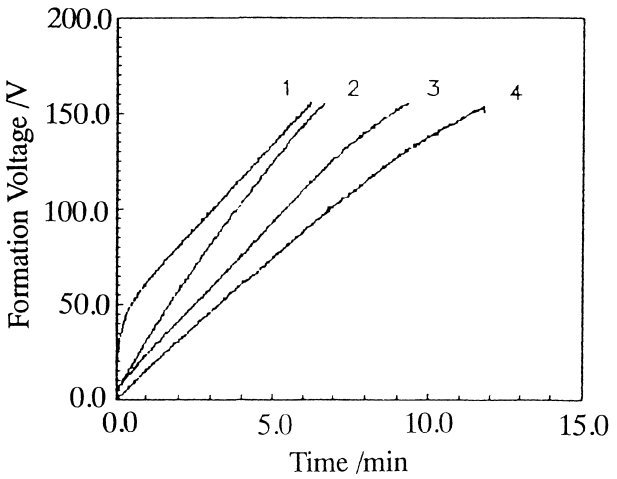

Fig. 4. Formation curves of sample B in different acidic solutions: (1) boric, (2) phosphoric, (3), citric and (4) sulfuric.

Table 2. Examination results of XRD

Samples	Main component phases	Other phases
A	Ti_2Al	Ti_3Al
B	TiAl	
C	$TiAl_3$	TiAl, Al (trace quantity)

films grow at the metal–oxide (M/O) interface by migration of O^{2-} ions inward and metal ions outward. Cabrera and Mott [9] suggested that the transmission of an ion from the metal into the oxide film at the M/O interface to form a cation interstitial could be the rate-determining step during film growth. Since the electronic energy states in these intermetallic phases are different, it is reasonable to suggest that the required energy to transmit a metal ion from the metal lattice into the oxide film at the M/O interface is different. When the required energy is lower, the metal ions can more promptly combine with O^{2-} ions to form oxides, that is, the oxide formation rate is higher. Otherwise, O^{2-} ions from the electrolytes will be surplus, which leads to oxygen evolution and then decreases the oxide formation rate. Therefore, samples A, B, and C with their different component phases, show different oxide formation rates (Figures 2 and 3).

3.2. *Electrolytic solutions*

In different electrolytic solutions, Al–Ti alloys had different anodic behaviours at the same current density. Figure 4 shows the formation curves of sample B in various acidic solutions of the same concentration (0.2 M) at 298 K. The formation curve in phosphoric solutions has the highest slope (dV/dt) and is almost linear. In boric solutions, the initial dV/dt is rather high, but soon declines while formation voltages over 50 V, that is to say, the V/t curves appear to inflect. As for the citric and sulfuric solutions, the slope of the formation curves are evidently both lower than that in phosphoric solutions. The main formation characteristics of sample B in these formation solutions are summarized in Table 3.

It is widely accepted that anodic oxide films are contaminated by acid anion species. The incorporation of anions in the formation of anodic oxide has a great effect on the growth of anodic films and the dielectric properties of the resulting films. In studies of aluminium anodization, Thompson and coworkers [10] proposed that the anodic oxide films are inhomogeneous and composed of an inner layer of pure alumina and an outer part contaminated by anion species. The ratio of the thickness of the anion-containing layer to that of the pure oxide layer is dependent on the electrolyte, which

Table 3. Formation characteristics of various acidic solutions and dielectric properties of their anodic oxide films

Electrolytic solution (0.2 M)	Time (up to 155 V) /min	Final formation current*/μA	Leakage current† /μA	CV of per unit areas ÿ/μF V cm^{-2}
Boric acid	6.23	43	26	8.14
Phosphoric acid	6.65	41	23	7.61
Citric acid	9.33	62	31	8.06
Sulfuric acid	11.83	120	40	7.66

* 150 V for 2 h potentiostatic.

† 0.01 vol % H_3PO_4 test solutions, 150 V for 10 min potentiostatic.

increases in the order chromic acid < phosphoric acid < oxalic acid < sulfuric acid. Further, the ionic conductivity is rather lower in the inner layer of pure alumina and higher in the outer layer contaminated by anion species due to its imperfections. Thus, during potentiostatic anodizing in the major anodizing acids, the larger the thickness of the anion-containing outer layer, the higher is the electric field strength at the inner layer and the larger is the oxide formation rate.

Similarly, during the anodic oxide growth of Al–Ti alloys, the phenomenon of anion incorporation into the growing oxide films also exists. It can be assumed that the films are also composed of an inner layer of relatively pure oxides and an outer layer incorporated by anions. The thickness ratio of the two layers varies with the respective acids. For example, the extent of anion incorporation into the films formed in sulfuric acid are the highest due to the ease of sulphate ion adsorption on the film surface, so the inner layer of the films is the thinnest. Because the anodic current density is identical in the case of galvanostatic anodization, the electric field strength across the inner layer of pure oxide is also identical in terms of Ohm's law. Further, the formation voltage drop occurs mainly across the inner layer owing to its lower ionic conductivity. Thus, the thicker the outer layer contaminated by anions, i.e. the thinner the inner layer of pure oxides, the lower is the voltage across the inner layer. Therefore, the lower dV/dt values of the formation curves in Figure 2 and the longer time needed to achieve 155 V for the formation voltage in Table 3, during anodizing at a given current density in electrolytes such as sulfuric acid, are expected due to their thinner pure oxide regions.

In addition, the incorporation of the acid anions into the growing oxides can also influence the structure and morphology of the anodic oxide films on Al–Ti alloys, and thus influence the dielectric properties of the films. As shown in Table 3, the leakage current of the films formed in phosphoric acid is the lowest, which is the key performance factor for electrolytic capacitor materials. Although the CV value per unit area is relative lower, it can still be considered that phosphoric acid is the best candidate electrolytic solution applied in Al–Ti alloy capacitors.

3.3. *Electrolyte temperatures*

Figure 5 shows the formation curve of sample B at different temperatures in 0.01 vol % phosphoric solutions. There is a great difference between these curves. During the experiment, it was observed that gas evolution on alloy samples intensified remarkably with increasing electrolyte temperature. That is to say, the formation efficiency of the anodic oxide declined and the release of oxygen increased. When the electrolyte temperature was increased to 80 °C, the formation voltage even appeared to give a negative increase (shown in Figure 5). Accordingly, the anodic oxide on Al–Ti alloy is unable to grow in high temperature solutions. In this

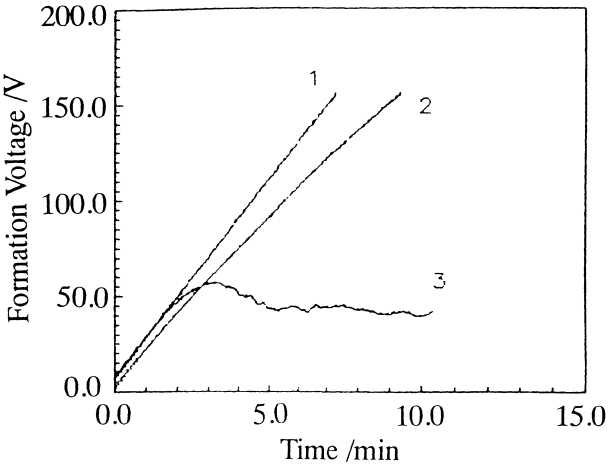

Fig. 5. Formation curves of sample B at different temperatures: (1) 25 °C, (2) 55 °C and (3) 80 °C.

case, the anodic processes are simply electrolysis of the solutions, and the release of oxygen on the alloy anode.

In reality, during anodic oxidation of alloy, the probable reactions are: metal dissolving into solution, oxide-forming, oxygen-evolving. In these reactions, which is predominant depends on the nature of the alloy and the anodizing conditions. It is well known that some valve metals, such as tantalum and aluminium, are anodized in high temperature solutions to form anodic oxide films which are used as dielectrics in electrolytic capacitors. This experiment has shown that the formation of anodic oxide at elevated temperature on pure titanium is difficult and its anodic oxide appears loose compared to that of tantalum or aluminium. So the anodic oxide films of titanium are unable to insulate the metal from the electrolytic solutions entirely. The electrons in titanium atoms, in fact, can take part in electrochemical reactions at the oxide–electrolyte (O/E) interface directly. On the contrary, the anodic oxide films of tantalum and aluminium are so dense that their electrical insulating property is very good. Transport of the electron can only occur through the oxide by a Poole-Frenkel or a tunnel mechanism [11]. Thus at the O/E interface, the generation of oxygen is difficult. Therefore, in higher temperature solutions, oxygen generation for the former is more intense, which inhibits the reaction of oxide formation. For the latter, due to the existence of dense barrier-type oxide films, the release of oxygen is inhibited but the rate of the oxide formation reaction increases with temperature. As for Al–Ti alloys, their oxide formation characteristics at elevated temperature appear similar to that of titanium because of the addition of titanium, that is, during Al–Ti alloy anodization in high temperature solutions, the oxygen release is so predominant that it inhibits oxide growth.

3.4. *Anodic current density*

It is obvious that an increase in anodic current density can increase the film growth rate, thereby increasing

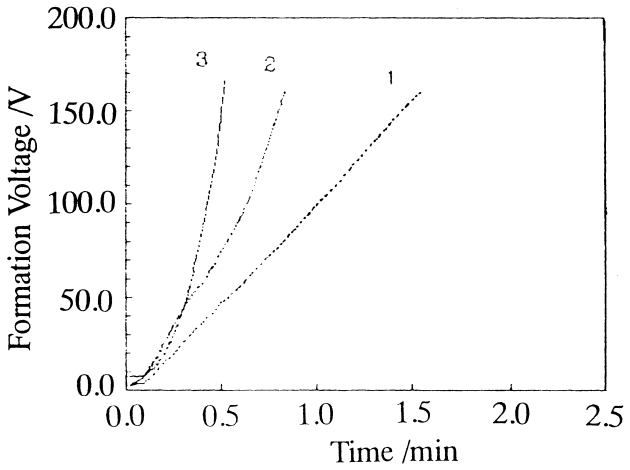

Fig. 6. Formation curves of sample B at different current densities: (1) 6, (2) 12 and (3) 24 mA/cm^{-2}.

dV/dt. Figure 6 also confirm this. Figure 6 shows the formation curves of sample B in 0.02 vol % phosphoric solutions at 298 K at different current densities. It was found during anodic tests that the rate of oxygen evolution was higher with the increasing current density. This phenomenon can be readily understood. According to the Butler–Volmer equation [12], it can be shown that the anodic oxidation current of oxygen evolution is as follows:

$$i_a \approx i^\circ \exp\left(\frac{\beta F \eta_a}{RT}\right)$$

where i° is exchange current density for oxygen generation, η_a is the anodic overpotential and β is the transfer coefficient.

As shown in Figure 6, the higher the anodic current density, the higher the formation voltage: in reality, the higher the overpotential of the anode. So the anodic oxygen current is higher; that is, the rate of oxygen evolution is higher.

3.5. *XPS*

Figure 7 and Figure 8(a1, a2) show the 2p XPS of titanium and aluminium before and after anodic oxidation of sample B alloy, respectively. The peaks of 2p electron binding energy of titanium and aluminium can be found from Figure 7. The Ti 2p peak of TiO_2 and Al 2p peak of Al_2O_3 are also present, resulting from the natural oxide films on the Al–Ti alloy surface. In addition, there is a difference between the peak position of the Al 2p electron binding energy for the alloys (71.50 eV, Figure 7(b)) and standard value (72.80 eV) for pure aluminium. The difference shows that the two elements in Al–Ti alloys do not simply blend with each other but form new alloy phases. This result is also in agreement with the above XRD experiments. After anodic oxidation, the peaks of aluminium and titanium disappear leaving the peaks of TiO_2 and Al_2O_3 only (compared with Figure 7 and Figure 8(a1, a2)). Moreover, compared with natural oxides, the peak position of TiO_2 and Al_2O_3 are not shifted and agree with standard spectra for TiO_2 and Al_2O_3 (within the scope of experimental error). This illustrates that anodic oxide films on sample B alloy are composed of TiO_2 and Al_2O_3. For sample A and C alloys, their XPS of the anodic oxide also have the same results (seen in Figure 8 (b1, b2, c1 and c2)). Therefore, the chemical composition of anodic oxide films on Al–Ti alloys can be expressed as $(TiO_2)_n(Al_2O_3)_m$, where n and m are parameters correlating with alloy composition. According to the following AES profiling analysis, results, the ratios of n:m for samples A, B, C can be calculated to be 0.88:1, 1.52:1 and 2.68:1, respectively.

3.6. *The depth profile of anodic oxide on alloys*

In fact, inert ion sputter profiling methods probably cause some artifacts such as preferential sputtering [13] of some elements in multicomponent oxides. Fortunately, sputtering yields of TiO_2 and Al_2O_3 are roughly equal [14]. So, AES (Auger electron spectroscopy) profiling analysis employing ion sputter methods can achieve accurate results for the chemical composition of these oxides.

As shown in Table 4, the proportion of aluminium and titanium are apparently different between the anodic oxide films on three sample alloys and in their matrix alloys. It is showed that the anodic oxidation probabilities of aluminium and titanium in the alloys are

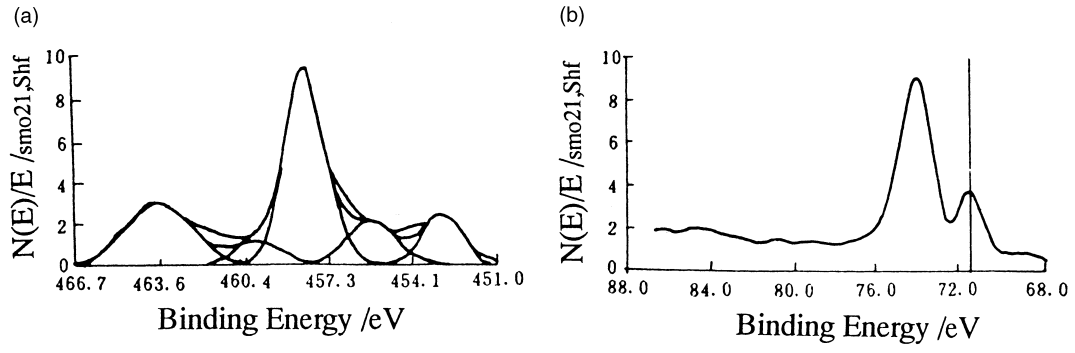

Fig. 7. The 2p XPS of titanium and aluminium before anodic oxidation of sample B: (a) titanium, (b) aluminium.

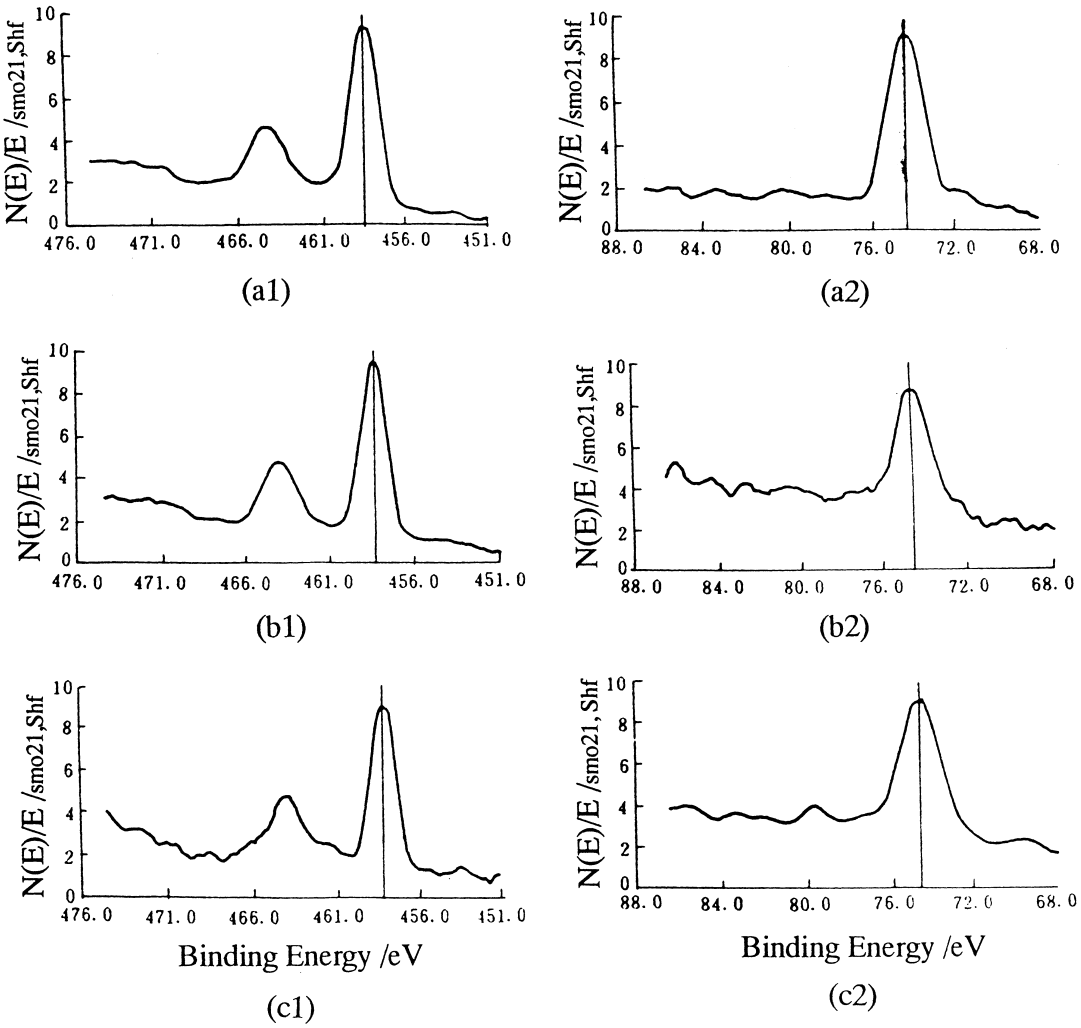

Fig. 8. The 2p XPS of titanium and aluminium after anodic oxidation of Al–Ti alloys. (a1), (b1) and (c1) are the 2p XPS of titanium of sample B, A and C, respectively; (a2), (b2) and (c2) are the 2p XPS of aluminium of sample B, A and C, respectively.

Table 4. AES profiling analysis results of anodic oxide films on Al–Ti alloys

Sputter time/min	1	1.5	2	2.5	3	3.5	Average
Sample A*	63	65	60	60	71	63	63.7
Sample B*	74	75	75	78	73	77	75.3
Sample C*	83	84	87	87	85	80	84.3

* The data are aluminium atom content (at %) in sum of aluminium and titanium atoms of anodic films.

not equal. If aluminium and titanium had the same anodic oxidation probability, the ratio of aluminium to titanium would be identical whether in anodic oxide films or in the alloy matrix. Since the ratios of aluminium in the oxide films for the three samples are all evidently higher than that in their matrix alloys, this indicates that the aluminium in alloys is preferentially oxidized. The reasons for this preferential oxidation may be as follows: (i) the activity of aluminium is higher than that of titanium. While the electrode is in the same polarized conditions, an aluminium atom loses its electrons more easily than a titanium atom. (ii) the radius and mass of Al^{3+} ions are both lower than that of Ti^{4+} ions [15], and thus the migration of Al^{3+} ions across the oxide films is more rapidly than that of Ti^{4+} ions in a high electric field. Consequently, the mobility of Al^{3+} ions should be higher than that of Ti^{4+} ions in oxide films. Actually, the transport number of Al^{3+} ions for pure aluminium during anodizing is also larger than that of Ti^{4+} ions for pure titanium [13].

In addition, Habazaki et al. have discussed the enrichment of alloying elements in studying the anodic oxidation of relatively dilute, metastable binary aluminium alloys [16]. They proposed that the enrichment of alloying elements in alloy layers could be correlated with the Gibbs free energy per equivalent for formation

of the alloying element oxides relative to that of alumina. The enrichment increases progressively for alloying elements associated with oxides of increasingly higher Gibbs free energy per equivalent, with no enrichment for alloying elements associated with oxides of lower Gibbs free energy per equivalent. Based on the above criteria, the titanium enrichment is expected since the Gibbs free energy per equivalent for formation of TiO_2 is higher than that of Al_2O_3. In other words, the aluminium is preferentially oxidized during anodizing of Al–Ti alloys.

4. Conclusion

The alloy composition had a significant influence on the anodic oxidation behaviour of Al–Ti alloys in acidic solutions. Under galvanostatic anodizing, the oxide formation rate for the Al–Ti alloy containing 54 at % aluminium was the highest and dielectric properties of its anodic oxide was also the best. In different electrolytic solutions, Al–Ti alloys had different anodic oxidation rates at the same current density. In this work, the formation rate of anodic oxide films on alloy in phosphoric solutions was the highest in the four acidic solutions. And the insulating property of its oxide films was also the best.

It was found that raising the solution temperature was disadvantageous to the growth of anodic films on Al–Ti alloys. In electrolytic solutions of high temperature (e.g., over 80 °C), the growth of the anodic oxide was inhibited. To obtain anodic oxide films having excellent dielectric properties, lower electrolyte temperatures should be chosen. In addition, by means of several surface analysis methods the chemical composition of films on Al–Ti alloys were determined as composites of TiO_2 and Al_2O_3, which can be expressed as $(TiO_2)_n(Al_2\ O_3)_m$, n and m are correlative with alloy composition. Furthermore, AES profiling analysis data for the Al–Ti alloys showed the preferential oxidation of aluminium.

Acknowledgements

The authors are very grateful to Professor Wanzhen Cao for her helpful discussions and also indebted to Northwestern Nonferrous Metals Academy for providing Al–Ti alloy samples.

References

1. H. Igarashi, S. Shimizu and Y. Kubo, *IEEE Trans. Compn. Hybrids & Manufacturing Techn.*, **CHM16**(4) (1983) 363.
2. S. Shimizu and Y. Arai, *European patent 84/102 880* (1984).
3. T. Mochizuki, *Japanese patent 88 306 614* (1988).
4. A.N. Kamkin, A.D. Davydov, *Prot. Met.* **35** (1999) 134.
5. Y. Li, H. Shimada, M. Sakairi, K. Shigyo, H. Takahashi and M. Seo, *J. Electrochem. Soc.* **144** (1997) 866.
6. G.M. Treacy, A.L. Rudd and C.B. Breslin, *J. Appl. Electrochem.* **30** (2000) 675.
7. H. Wu, X. Zhang and K.R. Hebert, *J. Electrochem. Soc.* **147** (2000) 2126.
8. G.E. Thompson and G.C. Wood, Anodic Films on Aluminium, *in* J.C. Scully (Ed.), 'Treatise on Materials Science and Technology', Vol. 23 (Academic Press, New York, 1983), p. 229.
9. N. Cabrera and N.F. Mott, *Rep. Prog. Phys.* **12** (1948) 163.
10. G.E. Thompson, R.C. Furneaux, G.C. Wood, J.A. Richardson and J.S. Goode, *Nature* **274** (1978) 433.
11. R. Coelho, 'Physics of Dielectrics' (Elsevier Scientific, Amsterdam, 1979).
12. Li Di, 'Principles of Electrochemistry' (Beijing Aviation University Press, Beijing, 1999).
13. A. Despic and V.P. Parkhutik, Electrochemistry of aluminium in aqueous solutions and physics of its anodic oxide, *in* J.O. Bockris, R.E. White and B.E. Conway (Eds), 'Modern Aspects of Electrochemistry', Vol. 20 (Plenum, New York, 1989), p. 449.
14. R. Kelly and N.Q. Lam, *Redat. Eff.* **19** (1973) 39.
15. R.C. Weast (Ed.), 'Handbook of Chemistry and Physics', 66th edition (CRC Press, Boca Raton, FL, 1985–1986) F164.
16. H. Habazaki, K. Shimizu, P. Skeldon, G.E. Thompson, G.C. Wood and X. Zhou, *Corros. Sci.* **39** (1997) 731.